



Cite this: *J. Mater. Chem. A*, 2022, 10, 5878

## Single-atom-based catalysts for photoelectrocatalysis: challenges and opportunities

Dong Liu, <sup>\*ab</sup> Xueying Wan,<sup>a</sup> Tingting Kong,<sup>c</sup> Weiwei Han<sup>c</sup> and Yujie Xiong <sup>\*b</sup>

Photoelectrocatalysis (PEC) has recently emerged as a promising strategy for utilizing solar energy due to its unique features in combining the merits of electrocatalysis and photocatalysis in solar energy harvesting, charge kinetics and catalytic reactions. However, it still encounters bottlenecks of scarce reaction sites and low product selectivity, restricting its development toward practical applications. Over the past decade, single-atom-based catalysts (SACs) with atomically dispersed metal sites have demonstrated immense potential in many catalytic reactions. In comparison with their nanoparticles (NPs) or bulk counterparts, the SACs normally have enormous surface active sites and trigger unique surface reactions, which, if rationally designed, can open up wide possibilities for PEC. Here, we overview the challenges and opportunities of SACs in PEC. We first summarize the advantages of SACs in enhancing the adsorption of reactants, charge transfer, catalytic selectivity, and catalytic activity. Then we discuss the rational design of single-atom active sites in the photoelectrochemical system. In the end, challenges and perspectives regarding the fundamental research and development of single-atom catalysts in PEC are also proposed. We foresee that this timely perspective can provide some important insights for researchers in this field and accelerate the development of PEC.

Received 25th September 2021  
Accepted 30th November 2021

DOI: 10.1039/d1ta08252c

[rsc.li/materials-a](https://rsc.li/materials-a)

<sup>a</sup>Suzhou Institute for Advanced Research, University of Science and Technology of China, Suzhou, Jiangsu 215123, China. E-mail: [dongliu@ustc.edu.cn](mailto:dongliu@ustc.edu.cn)

<sup>b</sup>Hefei National Laboratory for Physical Sciences at the Microscale, School of Chemistry and Materials Science, University of Science and Technology of China, Hefei, Anhui 230026, China. E-mail: [yjxiong@ustc.edu.cn](mailto:yjxiong@ustc.edu.cn)

<sup>c</sup>College of Chemistry and Chemical Engineering, Xi'an Shiyou University, Xi'an, Shaanxi 710054, China

## Introduction

The solar-to-chemical energy conversion has been regarded as one major solution to addressing current energy and environmental issues.<sup>1–3</sup> Stimulated by solar light, photogenerated electrons and holes can participate in redox reactions to realize



Dong Liu obtained his B.S. in chemical physics in 2012 and PhD in inorganic chemistry under the tutelage of Professor Yujie Xiong in 2017, both from the University of Science and Technology of China (USTC). From 2018 to 2021, he worked as a Postdoctoral Research Fellow at Nanyang Technological University, Singapore. He is currently a Research Professor at the USTC. His research interests

focus on developing a photo(electro)chemical system for solar-driven production of fuels and valuable chemicals.



Yujie Xiong received his B.S. in chemical physics in 2000 and PhD in inorganic chemistry in 2004, both from the University of Science and Technology of China (USTC). From 2004 to 2009, he worked as a Post-doctoral Fellow at the University of Washington in Seattle and as a Research Associate at the University of Illinois at Urbana-Champaign, respectively. He was the Principal Scientist of the

National Nanotechnology Infrastructure Network (NSF-NNIN) site at Washington University in St. Louis in 2009–2011. He joined the USTC faculty in 2011, and currently is the Chair Professor of Chemistry. His research centers on solar-driven artificial carbon cycle.

the energy conversion.<sup>4,5</sup> Solar-driven redox reactions are generally achieved *via* three pathways, *i.e.*, photocatalysis, photoelectrocatalysis, and photothermal catalysis. Photoelectrocatalysis (PEC) is a promising technology for solar-to-chemical energy conversion, which incorporates the merits of electrocatalysis and photocatalysis in solar energy harvesting, charge kinetics and catalytic reactions.<sup>5–7</sup> External bias or built-in photovoltage in the PEC system can promote the separation of photogenerated charges, invigorate the charges, increase their densities, and prolong their lifetimes. Abundant energetic photogenerated charges can activate reactants and motivate the chemical transformation. Nevertheless, PEC still encounters bottlenecks of scarce active sites and low catalytic selectivity, limiting its development.<sup>8–11</sup>

Single-atom-based catalysts (SACs) have recently emerged as a new class of catalysts with excellent activity and selectivity for various catalytic reactions,<sup>12–14</sup> which offer new opportunities for overcoming the limitations of the PEC system. The catalytic properties of SACs highly depend on the electronic structures of metal single atoms (SAs), the metal–support interaction, and the coordination environment.<sup>15</sup> These factors are critical to the adsorption, activation and catalytic reactions of reactants and intermediates in heterocatalysis. Maximal atom utilization efficiency and tunable density of single-atom sites ensure a sufficient quantity of active catalytic centers with cost effectiveness.<sup>16</sup> Furthermore, modulated electronic structures by tuning metal–support interaction bring vitality for the activation of adsorbed molecules and the catalytic reactions.<sup>17</sup> In the meantime, the specific adsorption configuration of small molecules on single-atom sites can regulate the selectivity of catalytic reactions.<sup>18,19</sup> Beyond enhancing the catalytic properties, establishing single-atom sites can also accelerate the charge separation and transfer in electrocatalysis and photocatalysis.

The photoelectrodes work as light-harvesting centers in the photoelectrochemical system and simultaneously catalyze chemical reactions with/without external bias.<sup>4</sup> The above-mentioned bottlenecks of PEC restrict the development toward practical applications. Correspondingly, SACs may provide a valuable solution to overcoming these bottlenecks of PEC on active sites and catalytic selectivity.<sup>12,20</sup> The introduction of SACs in PEC demands the rational design of photoelectrodes, and in turn, their composition and feasibility need to be fully considered.<sup>21,22</sup> By projecting the practicable scheme of SAC-coupled PEC, the high density of active sites and modulated electronic structures of SACs together with adequate photogenerated charges in PEC can notably boost the efficiency of solar-to-chemical energy conversion. As such, the activity and selectivity of photoelectrochemical reactions can be pertinently improved by the establishment of SACs in PEC.

To date, the application of SACs in PEC has been explored with only a few attempts.<sup>23–25</sup> Effectual integration of SACs in PEC still needs adequate research and precise regulation toward practical applications. This perspective summarizes the advantageous features of SACs in enhancing charge transfer, catalytic selectivity, and catalytic activity, which may compensate the shortcomings of general PEC reactions. Then recent

progress regarding single-atom-based photoelectrochemical applications will be summarized, and, on this basis, we propose potential design principles and strategies for future development of SACs in PEC. In the end, we discuss the challenges and perspectives regarding fundamental research and advances to provide insights and guidelines for this emerging field.

## Advantages of SACs for heterocatalysis

Heterocatalysis involves three essential steps: the adsorption of reactants from a fluid phase, the surface catalytic reaction of adsorbed species, and the desorption of products into the fluid phase. The total efficiency of heterocatalysis is determined by the efficiency of each step.<sup>26</sup> PEC is one type of heterocatalysis which contains similar steps for catalytic reactions as mentioned above. Specifically, directional adsorption of reactants, efficient charge separation and transfer, adequate activation of adsorbed species, selective catalytic transformation, and effective mass transfer are critical to the entire catalytic reaction. For these key steps in heterocatalysis, the unique geometric and electronic properties of SACs can play to their advantages.<sup>27</sup> SACs provide a powerful solution to achieve desirable chemical reactions with high activity and selectivity. This section will discuss the merits of SACs demonstrated in heterocatalysis, which can potentially take effect in photoelectrocatalysis.

### Modulated electronic structures

Electronic structures of catalysts are crucial to the overall catalytic process.<sup>28–30</sup> The adsorption bond strength of reactants or intermediates, the charge kinetics and the catalyst activity have been proven to be highly related to the characteristics of the surface electronic structure of catalysts.<sup>31,32</sup> After the metal SAs are anchored or coordinated with the support, the strong metal–support interaction can regulate the electronic structures of SAs due to the redistribution of charge density.<sup>33–35</sup> In the meantime, metal species and their oxidation states, coordination micro-environment and strain engineering can also affect the electronic structures of SACs, thereby altering the catalytic performance.<sup>34,35</sup> For instance, Lu *et al.* revealed the support effect on the electronic structures of Pt SA-based catalysts both experimentally and theoretically, and found that Pt atoms in Pt<sub>1</sub>/Co<sub>3</sub>O<sub>4</sub> had the largest 5d state depletion leading to extreme catalytic activity and excellent stability for hydrolytic dehydrogenation.<sup>36</sup> For solar-to-chemical energy conversion, Zhou *et al.* found that the deployment of Au SAs in Cd<sub>1–x</sub>S modulated the electronic structures of Au atoms, which could promote the charge transfer and offer sufficient electrons for photocatalytic CO<sub>2</sub> reduction reaction.<sup>30</sup> In another case, band engineering of Pt<sup>II</sup>–C<sub>3</sub>N<sub>4</sub> photocatalysts by introducing Pt SAs was proven to be an efficient solution to modify the band energy levels and shift the valence band maximum level to promote water oxidation.<sup>37</sup> Similarly, rational design of Ta<sub>3</sub>N<sub>5</sub> photoanodes by gradient Mg doping could improve the PEC water oxidation performance due to band engineering.<sup>38</sup> Overall, coupling the modulated electronic structures of SACs with the band engineering of

photoelectrodes will facilitate the PEC reactions by improving different steps of photoelectrocatalysis.

### Improved adsorption of reactants

Adsorption of reactants from a fluid phase is the first essential step in heterocatalysis. Generally, there are two forms of adsorption: chemisorption and physisorption, *via* chemical bonding or van der Waals forces between molecules and the catalyst surface, respectively. The strength and the orientation of chemisorption are critical for the subsequent activation and dissociation of adsorbed intermediates.<sup>39</sup> The geometry, composition, atomic arrangements and electronic structures of the catalysts, as well as the configuration of molecules, directly administrate the chemisorption process of reactants on the surface of the catalysts.<sup>40</sup> The incorporation of single metal atoms in SACs affects the symmetry of the d-band states and the filling due to the metal–support interaction. The unique electronic and structural properties in SACs can facilitate the strengthened and directional chemisorption of the reactants.<sup>41</sup> From the perspective of the electronic structure, SACs composed of different metals could lead to varied catalytic performance.<sup>32</sup> Parkinson *et al.* revealed the adsorption of the probe CO molecule on different model single-atom catalysts  $\text{Me}_1/\text{Fe}_3\text{O}_4$  (001) (Me: Cu, Ag, Au, Ni, Pd, Pt, Rh, or Ir) through experimental characterization studies and density functional theory (DFT) calculations.<sup>42</sup> Coordinating the metal atoms with a support alters their electronic structure. The charge transfer from different single metal sites to the support affects the d-states of the metal, the strength of the metal–CO bond and the adsorption energy of CO on single metal sites. In addition to the electronic structure, the unique geometric structure of SACs can also direct the adsorption of reactants on the atomically dispersed active sites. Ohno and Liu *et al.* inferred that the spatial and electronic features of SACs directly influenced the adsorption configuration of  $\text{O}_2$  molecules on atomically dispersed Sb, as shown in Fig. 1a and b, thereby affecting the reaction pathway and the selectivity of photocatalytic  $\text{O}_2$

reduction reaction.<sup>19</sup> In addition, first-principles simulation indicated that  $\text{CO}_2$  was adsorbed on isolated Cu sites with the adsorption energy of  $-0.463$  eV (Fig. 1c), while the adsorption of  $\text{CO}_2$  on the neighboring Cu pairs was noticeably weaker ( $-0.308$  eV) (Fig. 1d).<sup>18</sup> The rational design of SACs can offer favorable configurations and advantageous adsorption energy of chemisorbed molecules on single-atom active sites, to further improve the catalytic activity and selectivity of PEC.<sup>43</sup>

### Promoted charge separation and transfer

Anchored or coordinated with the support, single metal atoms can form strong interactions with their support.<sup>44</sup> The metal–support interaction arises with the orbital rehybridization and charge transfer across the interface. This strong metal–support interaction in SACs is beneficial to charge separation and transfer, which can redistribute the charge density around the metal sites with the formation of new chemical bonds.<sup>45</sup> Redistribution of d-band electrons and charge transfer between the SAs and the supports can stabilize the single active sites and boost the catalytic performances.<sup>46</sup> Sun and Botton *et al.* proved that charge transfer from the Pt SAs to the N atoms could generate unoccupied 5d orbital density of states of the Pt atoms, which was the reason for the excellent hydrogen evolution performance of Pt SAs/N-doped graphene nanosheets.<sup>47</sup> Adsorption and dissociation of molecules also benefit from the charge transfer from the single metal sites. The low O–O dissociation energy barrier and enhanced oxygen reduction reaction efficiency were attributed to the distinct charge transfer from the Nb SAs to the two O atoms, characterized by spin-polarized first-principles calculations, as illustrated in Fig. 2a.<sup>48</sup>

Promoted charge separation and transfer in SACs can provide sufficient charges to actuate the chemical reactions. Compared to Au nanoclusters distributed on the  $\text{Cd}_{1-x}\text{S}$  support, the hybridization between Au 5d and S 2p orbitals in Au–S bonds is substantially stronger for Au SAs/ $\text{Cd}_{1-x}\text{S}$ , which accelerates charge transfer on the surface and provides more sufficient electrons available for photocatalytic  $\text{CO}_2$  reduction

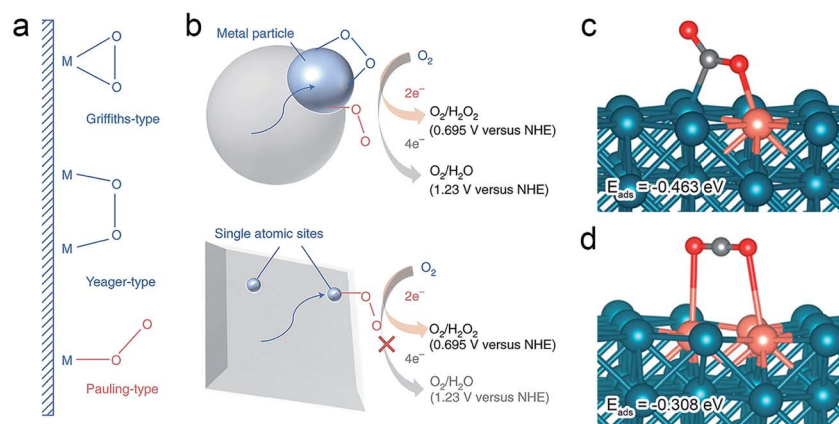


**Fig. 1** (a) Schematic structures of  $\text{O}_2$  adsorption on the metal surface. (b) Oxygen reduction reactions on a metal particle (top) and an isolated atomic site (bottom).<sup>19</sup> Reproduced with permission from ref. 19. Copyright 2021, Springer Nature. (c and d) First-principles simulation for the most favorable configurations and the corresponding adsorption energies of  $\text{CO}_2$  at an isolated Cu atom (c) and two neighboring Cu atoms (d).<sup>18</sup> Reproduced with permission from ref. 18. Copyright 2017, American Chemical Society.



Fig. 2 (a) Adsorption of  $O_2$  on single Nb sites and the corresponding electron density distribution with the charge flow from the Nb atom (blue) to the O atoms (yellow).<sup>48</sup> Reproduced with permission from ref. 48. Copyright 2013, Nature Publishing Group. (b) Scheme of single Au atoms in CdS with Cd or S vacancies with an alternative adsorption configuration.<sup>30</sup> Reproduced with permission from ref. 30. Copyright 2021, Springer Nature.

reaction, as shown in Fig. 2b.<sup>30</sup> In addition, the isolated single-atom active sites can trap photogenerated charges *via* chemical bonding in SACs, which reduces undesired charge recombination at the interface toward efficient photocatalysis.<sup>49</sup> Steady-state photoluminescence (PL) spectroscopy and surface photovoltage (SPV) spectroscopy can examine the charge separation, recombination and transfer process.<sup>50,51</sup> After introducing Co SAs onto partially oxidized graphene nanosheets or  $Bi_3O_4Br$  atomic layers, quenched PL intensity and enhanced SPV intensity were obtained, respectively, indicating increased charge separation and transfer efficiency regardless of different chemical bonds between single metal atoms and the support (Fig. 3).<sup>50,51</sup> As a technology combining the features of electrocatalysis and photocatalysis in solar energy harvesting, the efficiency of PEC highly depends on the separation of photogenerated charges and the charge transfer between the support and catalytically active sites.<sup>5</sup> SACs possessing the above advantages can exhibit competence in charge separation and transfer for efficient photoelectrocatalysis.

### Activation of reactants and selective catalytic reactions

Effective catalytic activation is the step following adsorption of reactants and charge transfer, which requires establishing



Fig. 3 (a) Scheme of single Co atoms coordinated on partially oxidized graphene nanosheets ( $Co_1-G$ ). (b) Steady-state PL spectra of an aqueous solution containing  $[Ru(bpy)_3]Cl_2$  with increasing  $Co_1-G$  nanosheets.<sup>50</sup> Reproduced with permission from ref. 50. Copyright 2018, John Wiley and Sons.

abundant active sites on the surface of catalysts. Isolated metal atoms in SACs are regarded as the primary active sites, which can enhance satisfactory adsorption and catalytic sites if rationally designed.<sup>17</sup> The density of isolated metal atoms is a key indicator to the catalytic reactions. SACs with tunable metal loading have been studied to achieve optimal catalytic performance and stability. An atomically dispersed Ir catalyst with 41.6 wt% metal loading was obtained by Wang *et al.* based on crosslinking and self-assembly of graphene quantum dots (QDs).<sup>52</sup> Numerous anchoring sites guarantee the sufficiency of active sites, and, at the same time, spacing between the dispersed metal atoms can prevent their aggregation. Specific surface area is a routine index to characterize a catalyst. For SACs, the surface area may not be that important in comparison with the performance. For example, introducing Sb SAs in polymer carbon nitride nanosheets reduced the surface area by 1/7.78 times, but the activity per area was greatly enhanced by more than 1900 times.<sup>19</sup> In addition to the number of active sites, the catalytic efficacy per active site also directs the overall catalytic performance of SACs. Turnover frequency (TOF) is a major parameter for evaluating the intrinsic activity per active site.<sup>50,53</sup> Owing to the unique coordination and electronic properties, SACs exhibit tens or hundreds of times higher TOF than the counterpart catalysts without single metal atoms. The TOF of  $Pd_1-Ti_{0.87}O_2$  with isolated Pd SAs is  $11\,110\ h^{-1}$  for Suzuki coupling reactions (Fig. 4a), more than 200 times that of  $PdCl_2$  and  $Pd(OAc)_2$  catalysts.<sup>54</sup> Hence it can be seen that SACs are competent for various catalytic reactions with tunable active sites and enhanced catalytic activity per site.

Catalysts generally perform by offering an alternative pathway involving an advantageous transition state and lower activation energy.<sup>57</sup> However, many catalytic reactions, such as  $CO_2$  reduction,  $O_2$  reduction, methane oxidation and biomass conversion, encounter problems of poor selectivity with complex products or over-reactions.<sup>55,58-60</sup> The regulation and optimization of selective catalytic reactions are significant to obtain the desired product in the industrial process. Improved adsorption and promoted charge transfer in SACs can facilitate the selective catalytic transformation by stabilizing the



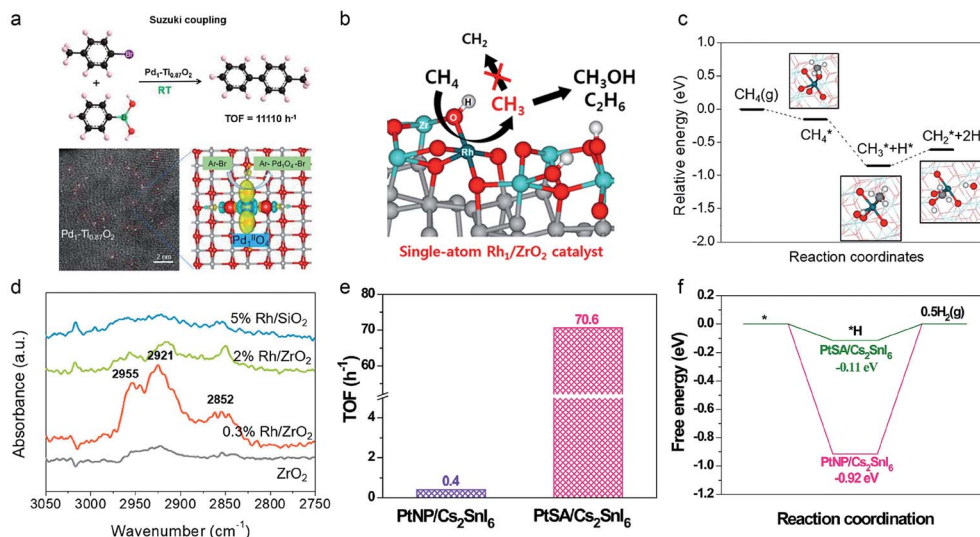


Fig. 4 (a) Scheme of the single-atom Pd site on the  $\text{Ti}_{0.87}\text{O}_2$  nanosheet for room-temperature Suzuki coupling reactions.<sup>54</sup> Reproduced with permission from ref. 54. Copyright 2021, Chinese Chemical Society. (b) Scheme of the single-atom Rh site on the  $\text{ZrO}_2$  catalyst for selective methane conversion. (c) Energy diagram of methane activation of the intermediates. (d) Diffuse reflectance infrared Fourier transform spectroscopy spectra (DRIFT) of  $\text{CH}_4$  adsorbed on bare  $\text{ZrO}_2$ , 0.3 wt%  $\text{Rh}/\text{ZrO}_2$  ( $\text{Rh}_1/\text{ZrO}_2$ ), 2 wt%  $\text{Rh}/\text{ZrO}_2$ , and 5 wt%  $\text{Rh}/\text{SiO}_2$ .<sup>55</sup> Reproduced with permission from ref. 55. Copyright 2017, American Chemical Society. (e) TOF and (f) calculated energy profile of  $\text{PtSA}/\text{Cs}_2\text{SnI}_6$  and  $\text{PtNP}/\text{Cs}_2\text{SnI}_6$  catalysts for photocatalytic  $\text{H}_2$  evolution, respectively.<sup>56</sup> Reproduced with permission from ref. 56. Copyright 2021, Springer Nature.

intermediates.<sup>17,61</sup> For example, stabilization of  $\text{CH}_3$  intermediates is crucial for direct methane conversion into value-added products. Cleavage of the first C–H bond of methane is the rate-determining step with the highest activation energy. Fig. 4b–d show the experimental results and DFT calculation of the selective methane conversion on  $\text{Rh}_1/\text{ZrO}_2$ , which confirmed that Rh SAs dispersed on the  $\text{ZrO}_2$  surface can effectively stabilize the  $\text{CH}_3$  intermediates and activate methane selectively compared to Rh NPs/ $\text{ZrO}_2$  catalysts.<sup>55</sup> In addition to stabilizing the intermediates, SACs can also lower the activation energy barrier and alter the selectivity of some representative catalytic reactions.<sup>57</sup> Anchoring  $\text{Pt}-\text{I}_3$  single-atom sites on all-inorganic  $\text{Cs}_2\text{SnI}_6$  perovskite can greatly reduce the energy barrier of hydrogen production to 0.11 eV, compared to that of Pt NPs on  $\text{Cs}_2\text{SnI}_6$  (0.92 eV), and the TOF was enhanced by 176.5-fold, as shown in Fig. 4e and f.<sup>56</sup> For solar-driven activation of  $\text{CO}_2$ , Co SAs/ $\text{Bi}_3\text{O}_4\text{Br}$  could energetically stabilize the  $\text{COOH}^*$  intermediates to increase the selectivity to CO, probed by *in situ* Fourier transform infrared (FTIR) spectroscopy.<sup>51</sup> DFT calculation indicated that the introduction of Co SAs could lower the  $\text{CO}_2$

activation energy barrier, and tune the rate-limiting step to  $\text{CO}^*$  desorption instead of  $\text{COOH}^*$  formation. As a result, the establishment of plentiful single-atom sites can particularly improve different steps in catalysis and boost the overall activity and selectivity, benefiting from the unique properties of SACs.<sup>62,63</sup>

## Progress of SACs for photoelectrocatalysis

Photoelectrocatalysis involves semiconductor-based photocatalysis with an applied bias or internal photovoltage. PEC combines the merits of electrocatalysis and photocatalysis in solar energy harvesting, charge kinetics and catalytic reactions into one integrated system.<sup>5,64</sup> Driven by solar light and external bias or internal photovoltage, the separation and transfer efficiency of photogenerated charges can be dramatically enhanced in PEC. Abundant photogenerated electrons and holes can activate chemical reactions, such as water splitting,  $\text{CO}_2$

Table 1 A summary of SACs for PEC applications

SACs	Substrate	Roles of SACs in PEC	PEC application	Improved performance	Reference
Ir-anion	$\text{NiO}_x/\alpha\text{-Fe}_2\text{O}_3$	Oxidation cocatalyst	Water oxidation	~2-fold	23
Co SAs	$g\text{-C}_3\text{N}_4/\text{PCS}$	Photoanode	Water oxidation	~5-fold	25
Ni-NC	$\alpha\text{-Fe}_2\text{O}_3$	Photoanode	Water oxidation	2.2-fold	69
Pt SAs	CdS	Photoanode	Enzyme-linked immunoassay		70
$\text{Pt}_1/\text{N}-\text{Ni}$	$\text{Cu}_2\text{O}$	Photocathode	Water reduction	4.7-fold	24
Ru SAs	$\text{Cu}_2\text{O}$	Cathode	$\text{N}_2$ reduction	~12-fold	71
CoPor- $\text{N}_3$	Carbon cloth	Photocathode	$\text{CO}_2$ reduction		72
Co SAs	Carbon	Cathode	$\text{N}_2$ reduction		73

reduction and biomass conversion, to realize artificial photosynthesis of high value-added chemicals.<sup>59,64,65</sup> However, in comparison with electrocatalysis and photocatalysis, scarce reaction sites and poor product selectivity restrict the development of PEC. Among many potential solutions, the deployment of SACs could bring new possibilities to PEC. Over the past decade, SACs have demonstrated immense potential in many catalytic reactions both experimentally and theoretically.<sup>66–68</sup> SACs exhibit unique advantages for promoting adsorption, activation and selective transformation of reactants, which may suit the remedy to the corresponding case in PEC. Inspired by the rational design and excellent performance of SACs in electrocatalysis and photocatalysis, the first single-atom-based PEC reaction was revealed in 2017.<sup>23</sup> Nevertheless, the application of SACs in the PEC system is still rare. The progress of SACs in PEC will be discussed in further detail below (Table 1).

Cui *et al.* first reported atomically dispersed Ni–Ir sites for PEC oxygen evolution in 2017. Soluble monomeric hexahydroxyiridate  $[\text{Ir}(\text{OH})_6]^{2-}$  anions could electrostatically adsorb to the positively charged  $\text{NiO}_x$  sites anchored on the hematite film photoanode (Fig. 5a and b).<sup>23</sup> In such a PEC system, the photocurrent density was increased by about 2-fold at 1.23 V vs. RHE, and the onset potential was reduced by about 200 mV after the creation of Ni–Ir sites in the hematite photoanode. Atomically dispersed Ni sites acted as a movable bridge for continuous hole transfer from the hematite support to the Ir center. As a result, enhanced solar-driven oxygen evolution performance with a faradaic yield of 94% was achieved after rationally integrating the soluble molecular catalysts with atomically dispersed  $\text{NiO}_x$  in a PEC system. Similarly, modifying single Ni sites/carbon nanosheets on the  $\alpha\text{-Fe}_2\text{O}_3$  photoanode could facilitate charge separation and transfer at the interface and provide sufficient active sites for oxygen evolution (Fig. 5c).<sup>69</sup> In parallel to the metal oxide semiconductor support, single metal

atoms can also bridge porous carbon spheres (PCS) with graphitic carbon nitride ( $\text{g-C}_3\text{N}_4$ ), as illustrated in Fig. 5d.<sup>25</sup> The strong coupling effect of PCS/Co SAs/ $\text{g-C}_3\text{N}_4$ , together with promoted charge separation/transfer and improved surface reaction dynamics, resulted in enhanced PEC water splitting activity.

SACs can also be utilized for PEC reduction reactions.<sup>71–73</sup> As shown in Fig. 6a and b, the  $\text{Cu}_2\text{O}$  nanowire (NW) photocathode has been retrofitted with  $\text{Pt}_1/\text{N-Ni}$  (Pt SAs supported by a porous nickel framework on nickel foam) as a co-catalyst for hydrogen production.<sup>24</sup> In comparison with pristine  $\text{Cu}_2\text{O}$  NW and Pt NP decorated N-Ni/ $\text{Cu}_2\text{O}$  NW photocathodes, the photocurrent density of the  $\text{Pt}_1/\text{N-Ni}/\text{Cu}_2\text{O}$  NW photocathode was increased by about 4.7 and 2 times for PEC water reduction, respectively. The  $\text{Pt}_1/\text{N-Ni}/\text{Cu}_2\text{O}$  NW photocathode could produce a high photocurrent density of  $11.9 \text{ mA cm}^{-2}$  at 0 V vs. RHE and a high photo-to-hydrogen conversion efficiency of 1.75% due to the low charge transfer resistance at the interface and excellent electrochemical hydrogen evolution activity of the  $\text{Pt}_1/\text{N-Ni}$  co-catalyst. It is worth noting that SACs can also work in a photoelectrochemical biosensing platform to perform an enzyme-free immunosorbent assay.<sup>70</sup> Anchoring Pt SAs on CdS nanorods could remarkably enhance the photoelectrochemical biosensing signal. The strong metal–support interaction between Pt SAs and the CdS nanorod support alters the charge distribution and increases the charge density of CdS, thereby promoting the charge separation and transfer. As a result, the Pt SA–CdS nanorod photoelectrode showed excellent photoelectrochemical detection sensitivity and selectivity.

To better understand the mechanisms, photoelectrochemical measurements have been investigated to assess the separation and transfer of photogenerated charges of photocatalysts. Introduction of SACs to photocatalysts can effectively suppress the recombination of photogenerated charges, thereby increasing the photocurrent density. For example,

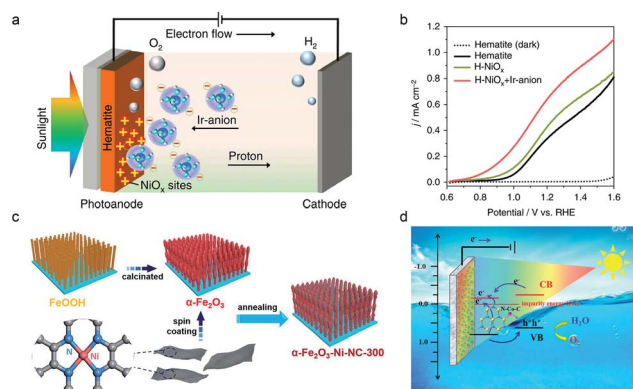


**Fig. 5** (a) Schematic illustration of the preparation process of the Ni–Ir site-based PEC system. Reproduced with permission from ref. 23. Copyright 2017, Springer Nature. (b) Linear sweep voltammograms of different photoanodes under AM 1.5 irradiation.<sup>23</sup> (c) Scheme of fabrication procedures for  $\alpha\text{-Fe}_2\text{O}_3$  and  $\alpha\text{-Fe}_2\text{O}_3\text{-Ni-NC-300}$  films.<sup>69</sup> Reproduced with permission from ref. 69. Copyright 2017, John Wiley and Sons. (d) The performance enhancement mechanism of PCS/Co SAs/ $\text{g-C}_3\text{N}_4$ .<sup>25</sup> Reproduced with permission from ref. 25. Copyright 2019, Elsevier.

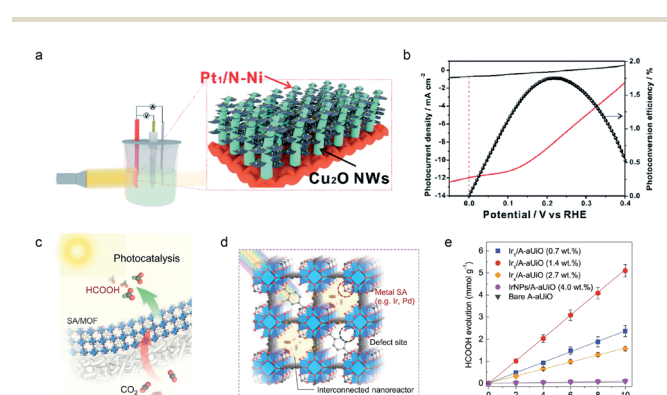


**Fig. 6** (a) Schematic illustration and (b) PEC performance of  $\text{Pt}_1/\text{N-Ni}/\text{Cu}_2\text{O}$  NWs for water reduction.<sup>24</sup> Reproduced with permission from ref. 24. Copyright 2021, The Royal Society of Chemistry. The scheme of the (c) MOF membrane and (d) MOF structures with single metal atoms for photocatalytic  $\text{CO}_2$  reduction. (e) Time course of  $\text{HCOOH}$  evolution on A-aUiO, Ir<sub>1</sub>/A-aUiO, Ir<sub>x</sub>/A-aUiO and IrNPs/A-aUiO catalysts.<sup>74</sup> Reproduced with permission from ref. 74. Copyright 2021, Springer Nature.

Wang *et al.* demonstrated that Ir SAs/NH<sub>2</sub>-UiO-66 (A-aUiO) metal-organic framework (MOF) membranes could effectively and selectively actuate CO<sub>2</sub> photoreduction to HCOOH (Fig. 6c–e).<sup>74</sup> An enhanced photocurrent density was obtained by the Ir species/A-aUiO depositing photoelectrode compared to pristine A-aUiO. When the size of Ir species was shrunk from nanoparticles to clusters (Ir<sub>x</sub>) and single atoms (Ir<sub>1</sub>), the formic acid evolution rate increased from 0.01 mmol g<sub>cat</sub><sup>-1</sup> h<sup>-1</sup> to 0.16 mmol g<sub>cat</sub><sup>-1</sup> h<sup>-1</sup> and 0.51 mmol g<sub>cat</sub><sup>-1</sup> h<sup>-1</sup>, and the selectivity of HCOOH was improved from 16.5% to 79.8% and nearly 100%, respectively. Similarly, Ag, Au, Pt, Co and Er SAs supported by g-C<sub>3</sub>N<sub>4</sub>, MOFs/covalent organic frameworks (COFs), TiO<sub>2</sub>, CdS and other semiconductor nanomaterials could boost the photocurrent density and the total photocatalytic performance compared to their counterparts without single metal active sites.<sup>30,49,75–83</sup> From these few cases, SACs have demonstrated their potentials in PEC applications. The rational deployment and fundamental investigation of SACs in PEC deserve further study.

## Challenges and opportunities of SACs for photoelectrocatalysis

As mentioned in the preceding sections, SACs exhibit unique properties in heterocatalysis.<sup>20</sup> Outstanding catalytic performance with maximal atom utilization efficiency and cost effectiveness make SACs promising in practical industrial processes. To realize solar-to-chemical transformation, PEC is a technology for competently utilizing solar energy and upgrading chemicals.<sup>9</sup> Proven by experimental results and theoretical simulations, the implementation of SACs may remedy the deficiencies of PEC in scarce reaction sites and poor selectivity. Some studies have achieved the application of SACs in PEC according to recent reports. However, the integration of SACs in PEC still encounters practical challenges. For this reason, this perspective will propose some potential solutions and outlook for the development of SACs in PEC in this section.

### Design of SACs in photoelectrodes

SACs with atomically dispersed metal sites need to be braced and stabilized by the support. The electronic and catalytic properties of SACs are determined by the coordination

environment of the support and the metal atoms. Rational design and precise modulation of SACs are critical to PEC reactions, since the morphology and composition will directly influence the surface and electronic properties of SACs, thus affecting the adsorption and activation of reactants as well as the overall activity and selectivity of catalytic reactions. Fig. 7 shows two main strategies for designing SAC based photoelectrodes in PEC. The first approach is the deployment of SACs as a photoelectrode (Fig. 7a). The main module of the PEC system is the photoelectrode, which is usually a semiconductor grown on a conductive substrate, such as TiO<sub>2</sub> nanowires and BiVO<sub>4</sub> nanoarrays on fluorine-doped tin oxide (FTO) glasses.<sup>59,84</sup> The selection of the support of SACs is one of the key factors for the operative integration of SACs in PEC (Fig. 7a). Establishing SACs in the PEC system requires semiconductor supports grown on conductive substrates, which not only stabilize SACs but also absorb solar light to generate electron-hole pairs and transfer charges. Single metal atoms can be supported by many typical metal oxide supports, such as Fe<sub>2</sub>O<sub>3</sub>, TiO<sub>2</sub>, WO<sub>3</sub>, ZnO and indium tin oxide.<sup>67,85–90</sup> These semiconductor metal oxide materials can be used as photoelectrodes when fabricated on the conductive substrate, in the shape of films, nanowires, nanoflakes and others. Subsequently, the single metal atoms can be deployed on the surface of these semiconductor supports by wet chemical strategies or pyrolysis methods. Strong metal-support interactions between the single metal atoms and the semiconductor metal oxide supports will lead to the redistribution of electrons and promote charge transfer.<sup>91</sup> Predictably, the introduction of atomically dispersed metal atoms to the semiconductor metal oxide supports as photoelectrodes can effectively increase the number of active sites, enhance catalytic efficacy per active site, and improve the adsorption of reactants and charge transfer, while maintaining the light absorption ability and adequate photogenerated charges.

In addition to the metal oxide support, g-C<sub>3</sub>N<sub>4</sub> is another competent semiconductor support for applying SACs for PEC. SAC based g-C<sub>3</sub>N<sub>4</sub> photocatalysts possess excellent photocatalytic performance.<sup>92</sup> The synthetic approaches of g-C<sub>3</sub>N<sub>4</sub> supported SACs are much simpler to operate than metal oxide supported SACs, while growing the g-C<sub>3</sub>N<sub>4</sub> film on a conductive substrate is tricky but achievable. The flexible surface and tunable coordination environment of g-C<sub>3</sub>N<sub>4</sub> as well as the tunable single metal centers can bring more possibilities to PEC

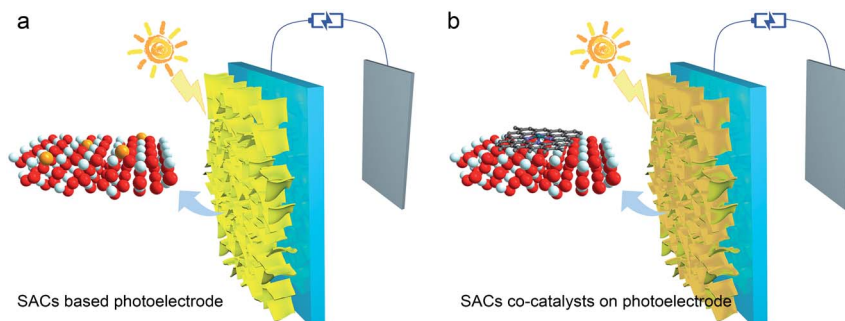


Fig. 7 Schematic illustration of the (a) SAC based photoelectrode and (b) SAC co-catalysts on the photoelectrode in PEC.

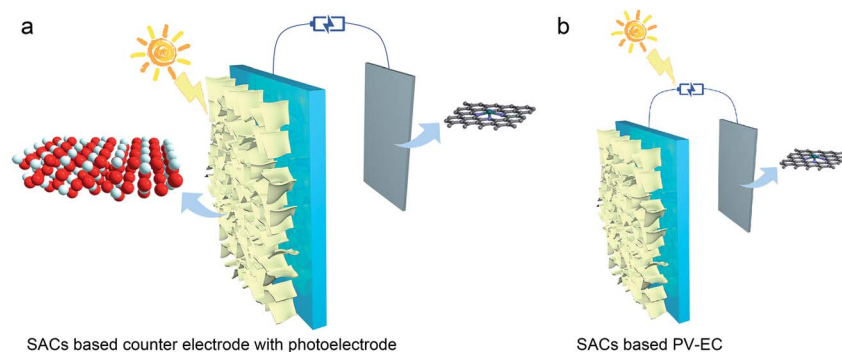


Fig. 8 Schematic illustration of the (a) SAC based counter electrode in PEC and (b) SAC based PV-EC system.

applications. In addition to being employed as the photoelectrode, SACs can act as the co-catalysts for redox reactions when rationally deposited on photoelectrodes (Fig. 7b). Graphene and MOFs/COF based SACs have been verified noticeably active for many redox reactions.<sup>93–95</sup> Graphene or MOFs/COF derived carbon materials can provide conductive channels to facilitate the charge transfer to the single metal active sites. Bridging the light absorbing photoelectrodes with the reactants, SAC based co-catalysts will trap photogenerated charges from the photoelectrodes, thus actuating the redox reactions.<sup>14,77</sup> The improved adsorption and activation of reactants and promoted charge transfer and selective catalytic reactions by SAC based co-catalysts can enhance the overall activity and selectivity of PEC reactions.<sup>89</sup> In general, rational design of SACs in photoelectrodes by composing SACs as one component of photoelectrodes or utilizing SACs as co-catalysts can integrate their advantages into the PEC system and significantly boost the PEC performance.

### Scheme of the SAC based PEC system

Besides the creation of SACs on photoelectrodes, there exist other approaches to optimize the PEC system. A PEC system is usually composed of two photoelectrodes, or one photoelectrode and one counter electrode. The reactions at the counter electrodes affect the overall performance. As reported, optimized anodic electro-oxidation could lower the working potential for CO<sub>2</sub> electroreduction and lower the electricity consumption by up to 53%.<sup>96</sup> SACs exhibited excellent catalytic activity and selectivity in electrocatalytic reactions, which can be applied as the counter electrodes to reduce the overpotential and enhance the total production efficiency and economic viability, as illustrated in Fig. 8a.<sup>73</sup> For example, the typical anodic reaction in the PEC CO<sub>2</sub> reduction system is the oxygen evolution reaction (OER). SACs can optimize the reaction pathway with lower activation energy barriers and improve the activity for the OER. The coupling of SACs as counter electrodes will boost the overall performance of the PEC CO<sub>2</sub> reduction system. Photovoltaic-electrocatalysis (PV-EC) is another feasible strategy to realize solar-to-chemical transformation using SACs (Fig. 8b).<sup>97,98</sup> Analogous to the roles in PEC, SACs can work as active sites on the electrodes to drive anodic and

cathodic reactions in a PV-EC system, thus improving the overall catalytic performance.

### Challenges of the SAC based PEC system

From the perspective of practical applications, the adaptability of the metal and support, the fabrication feasibility and the stability are the main challenges for applying SACs in PEC. Based on experimental and theoretical studies, the composition, configuration and coordination environment of metal sites and photoactive semiconductor supports are vital for the SAC based PEC reactions. The coupling effect of strong metal-support interaction and photogenerated charge migration will influence the adsorption and activation of reactants on single metal sites. In-depth studies of the working mechanisms through advanced spectroscopy and theoretical simulation are needed to fundamentally understand the different steps of SAC based PEC applications.<sup>99</sup> For manufacturing SACs in PEC, one needs to consider the adaptability and the fabrication feasibility of growing semiconductor supports on conductive substrates and the establishment of atomically dispersed metal atoms on the surface. Reasonably regulating wet chemical and thermal treatment routes can realize the fabrication and effective integration of atomically dispersed metal atoms in PEC. Besides, SACs in PEC confront possible photocorrosion, while effective coordination and strong stabilization by the support can stabilize the atomically dispersed metal atoms.<sup>100</sup>

## Conclusion and outlook

Photoelectrocatalysis is one potent strategy of artificial photosynthesis to harvest solar energy and upgrade chemicals. Practical applications toward industrial processes demand catalytic reactions with high activity, selectivity, stability and cost effectiveness in PEC. Much effort has been devoted to advancing the development of PEC. As mentioned above, SACs, a rising star in the field of catalysis, possess unique geometric and electronic properties.<sup>67</sup> The deployment of SACs in the PEC system is a promising solution to resolving the current issues in terms of reaction sites and product selectivity. Improved chemisorption of reactants, promoted charge separation and transfer, optimal reaction pathway, selective catalytic reaction and maximal atom utilization efficiency by SACs can definitely boost the overall



catalytic and economic efficiency of PEC as proven by experimental and theoretical results. These properties highly depend on the composition and configuration of SACs and the interaction between the support and metal sites. Effective integration and rational design of SACs are critical to the overall performance of PEC. Therefore, efforts should be made to rationalize and develop SAC based PEC systems to further achieve efficient artificial photosynthesis.

Based on structural design and performance optimization, it is imperative to achieve in-depth understanding on SAC based PEC. One needs to confirm the structure–function relationships between the SAC based photoelectrodes and the catalytic performance. The extracted structure–function relationships can guide the optimal design of SAC based PEC systems. SAC based PEC reactions involve complex steps, including directional adsorption of reactants, charge redistribution, alternative reaction pathways and selective catalytic reactions. Advanced characterization and theoretical simulation studies are required to comprehensively explore these critical steps, to further optimize SAC based PEC. On this basis, novel device design can realize the effectual utilization of SACs in PEC.

Overall, the implementation of SACs will provide optimal enhancement of catalytic activity and selectivity to compensate for the corresponding shortcomings of PEC. The unique advantages of SACs ensure their promising future applications, particularly for solar-to-chemical transformation. We hope that this perspective highlighting the challenges and opportunities of SACs for PEC will bring new insights and inspire new ideas for this research field.

## Conflicts of interest

There are no conflicts to declare.

## Acknowledgements

This work was financially supported in part by the National Key R&D Program of China (2020YFA0406103), NSFC (21725102, 51902253, 91961106, and 22005242), CAS Hundred Talent Program, and the Shaanxi Provincial Natural Science Foundation (2020JQ-778).

## References

- 1 T. P. Yoon, M. A. Ischay and J. Du, *Nat. Chem.*, 2010, **2**, 527–532.
- 2 P. Christopher, H. Xin, A. Marimuthu and S. Linic, *Nat. Mater.*, 2012, **11**, 1044–1050.
- 3 B. Wang, G. M. Biesold, M. Zhang and Z. Lin, *Chem. Soc. Rev.*, 2021, **50**, 6914–6949.
- 4 V. Augugliaro, G. Camera-Roda, V. Loddo, G. Palmisano, L. Palmisano, J. Soria and S. Yurdakal, *J. Phys. Chem. Lett.*, 2015, **6**, 1968–1981.
- 5 A. Paracchino, V. Laporte, K. Sivula, M. Gratzel and E. Thimsen, *Nat. Mater.*, 2011, **10**, 456–461.
- 6 F. X. Xiao, J. Miao, H. B. Tao, S. F. Hung, H. Y. Wang, H. B. Yang, J. Chen, R. Chen and B. Liu, *Small*, 2015, **11**, 2115–2131.
- 7 T. Li, J. He, B. Pena and C. P. Berlinguette, *Angew. Chem., Int. Ed.*, 2016, **55**, 1769–1772.
- 8 Y. Yang, S. Wang, Y. Jiao, Z. Wang, M. Xiao, A. Du, Y. Li, J. Wang and L. Wang, *Adv. Funct. Mater.*, 2018, **28**, 1805698.
- 9 N. Zhang, R. Long, C. Gao and Y. Xiong, *Sci. China Mater.*, 2018, **61**, 771–805.
- 10 M. Nazemi and M. A. El-Sayed, *Nano Energy*, 2019, **63**, 103886.
- 11 S. Zhou, K. Sun, J. Huang, X. Lu, B. Xie, D. Zhang, J. N. Hart, C. Y. Toe, X. Hao and R. Amal, *Small*, 2021, **17**, e2100496.
- 12 X. Cui, W. Li, P. Ryabchuk, K. Junge and M. Beller, *Nat. Catal.*, 2018, **1**, 385–397.
- 13 X. Li, X. Yang, Y. Huang, T. Zhang and B. Liu, *Adv. Mater.*, 2019, **31**, 1902031.
- 14 C. Gao, J. Low, R. Long, T. Kong, J. Zhu and Y. Xiong, *Chem. Rev.*, 2020, **120**, 12175–12216.
- 15 S. Mitchell, E. Vorobyeva and J. Perez-Ramirez, *Angew. Chem., Int. Ed.*, 2018, **57**, 15316–15329.
- 16 Y. Chen, S. Ji, C. Chen, Q. Peng, D. Wang and Y. Li, *Joule*, 2018, **2**, 1242–1264.
- 17 M. D. Marcinkowski, M. T. Darby, J. Liu, J. M. Wimble, F. R. Lucci, S. Lee, A. Michaelides, M. Flytzani-Stephanopoulos, M. Stamatakis and E. C. H. Sykes, *Nat. Chem.*, 2018, **10**, 325–332.
- 18 R. Long, Y. Li, Y. Liu, S. Chen, X. Zheng, C. Gao, C. He, N. Chen, Z. Qi, L. Song, J. Jiang, J. Zhu and Y. Xiong, *J. Am. Chem. Soc.*, 2017, **139**, 4486–4492.
- 19 Z. Teng, Q. Zhang, H. Yang, K. Kato, W. Yang, Y.-R. Lu, S. Liu, C. Wang, A. Yamakata, C. Su, B. Liu and T. Ohno, *Nat. Catal.*, 2021, **4**, 374–384.
- 20 X. F. Yang, A. Wang, B. Qiao, J. Li, J. Liu and T. Zhang, *Acc. Chem. Res.*, 2013, **46**, 1740–1748.
- 21 H. Xu, D. Cheng, D. Cao and X. C. Zeng, *Nat. Catal.*, 2018, **1**, 339–348.
- 22 B. Peng, H. Liu, Z. Liu, X. Duan and Y. Huang, *J. Phys. Chem. Lett.*, 2021, **12**, 2837–2847.
- 23 C. Cui, M. Heggen, W. D. Zabka, W. Cui, J. Osterwalder, B. Probst and R. Alberto, *Nat. Commun.*, 2017, **8**, 1341.
- 24 S. Tong, B. Fu, L. Gan and Z. Zhang, *J. Mater. Chem. A*, 2021, **9**, 10731–10738.
- 25 Q. Song, J. Li, L. Wang, Y. Qin, L. Pang and H. Liu, *J. Catal.*, 2019, **370**, 176–185.
- 26 M. E. Davis and R. J. Davis, *Fundamentals of Chemical Reaction Engineering*, McGraw-Hill, New York, NY, 2003.
- 27 T. Chen, L. Ye and T. W. B. Lo, *J. Mater. Chem. A*, 2021, **9**, 18773–18784.
- 28 X. Du, J. Huang, J. Zhang, Y. Yan, C. Wu, Y. Hu, C. Yan, T. Lei, W. Chen, C. Fan and J. Xiong, *Angew. Chem., Int. Ed.*, 2019, **58**, 4484–4502.
- 29 C. M. Tian, M. Jiang, D. Tang, L. Qiao, H. Y. Xiao, F. E. Oropeza, J. P. Hofmann, E. J. M. Hensen, A. Tadich, W. Li, D. C. Qi and K. H. L. Zhang, *J. Mater. Chem. A*, 2019, **7**, 11895–11907.

- 30 Y. Cao, L. Guo, M. Dan, D. E. Doronkin, C. Han, Z. Rao, Y. Liu, J. Meng, Z. Huang, K. Zheng, P. Chen, F. Dong and Y. Zhou, *Nat. Commun.*, 2021, **12**, 1675.
- 31 J. Greeley, J. K. Nørskov and M. Mavrikakis, *Annu. Rev. Phys. Chem.*, 2002, **53**, 319–348.
- 32 A. Nilsson, L. G. M. Pettersson, B. Hammer, T. Bligaard, C. H. Christensen and J. K. Nørskov, *Catal. Lett.*, 2005, **100**, 111–114.
- 33 W. H. Lai, Z. Miao, Y. X. Wang, J. Z. Wang and S. L. Chou, *Adv. Energy Mater.*, 2019, **9**, 1900722.
- 34 G. Meng, J. Zhang, X. Li, D. Wang and Y. Li, *Appl. Phys. Rev.*, 2021, **8**, 021321.
- 35 Y. Zhu, W. Peng, Y. Li, G. Zhang, F. Zhang and X. Fan, *Small Methods*, 2019, **3**, 1800438.
- 36 J. Li, Q. Guan, H. Wu, W. Liu, Y. Lin, Z. Sun, X. Ye, X. Zheng, H. Pan, J. Zhu, S. Chen, W. Zhang, S. Wei and J. Lu, *J. Am. Chem. Soc.*, 2019, **141**, 14515–14519.
- 37 H. Su, W. Che, F. Tang, W. Cheng, X. Zhao, H. Zhang and Q. Liu, *J. Phys. Chem. C*, 2018, **122**, 21108–21114.
- 38 Y. Xiao, C. Feng, J. Fu, F. Wang, C. Li, V. F. Kunzelmann, C.-M. Jiang, M. Nakabayashi, N. Shibata, I. D. Sharp, K. Domen and Y. Li, *Nat. Catal.*, 2020, **3**, 932–940.
- 39 M. M. Millet, G. Algara-Siller, S. Wrabetz, A. Mazheika, F. Girgsdies, D. Teschner, F. Seitz, A. Tarasov, S. V. Levchenko, R. Schlogl and E. Frei, *J. Am. Chem. Soc.*, 2019, **141**, 2451–2461.
- 40 M. D. Hossain, Y. Huang, T. H. Yu, W. A. Goddard III and Z. Luo, *Nat. Commun.*, 2020, **11**, 2256.
- 41 Z. Jakub, J. Hulva, M. Meier, R. Bliem, F. Kraushofer, M. Setvin, M. Schmid, U. Diebold, C. Franchini and G. S. Parkinson, *Angew. Chem., Int. Ed.*, 2019, **58**, 13961–13968.
- 42 J. Hulva, M. Meier, R. Bliem, Z. Jakub, F. Kraushofer, M. Schmid, U. Diebold, C. Franchini and G. S. Parkinson, *Science*, 2021, **371**, 375–379.
- 43 W. Guo, Z. Wang, X. Wang and Y. Wu, *Adv. Mater.*, 2021, **33**, 2004287.
- 44 B. Han, Y. Guo, Y. Huang, W. Xi, J. Xu, J. Luo, H. Qi, Y. Ren, X. Liu, B. Qiao and T. Zhang, *Angew. Chem., Int. Ed.*, 2020, **59**, 11824–11829.
- 45 P. Hu, Z. Huang, Z. Amghouz, M. Makkee, F. Xu, F. Kapteijn, A. Dikhtiarenko, Y. Chen, X. Gu and X. Tang, *Angew. Chem., Int. Ed.*, 2014, **53**, 3418–3421.
- 46 B. Qiao, J.-X. Liang, A. Wang, C.-Q. Xu, J. Li, T. Zhang and J. J. Liu, *Nano Res.*, 2015, **8**, 2913–2924.
- 47 N. Cheng, S. Stambula, D. Wang, M. N. Banis, J. Liu, A. Riese, B. Xiao, R. Li, T. K. Sham, L. M. Liu, G. A. Botton and X. Sun, *Nat. Commun.*, 2016, **7**, 13638.
- 48 X. Zhang, J. Guo, P. Guan, C. Liu, H. Huang, F. Xue, X. Dong, S. J. Pennycook and M. F. Chisholm, *Nat. Commun.*, 2013, **4**, 1924.
- 49 X. Fang, Q. Shang, Y. Wang, L. Jiao, T. Yao, Y. Li, Q. Zhang, Y. Luo and H. L. Jiang, *Adv. Mater.*, 2018, **30**, 1705112.
- 50 C. Gao, S. Chen, Y. Wang, J. Wang, X. Zheng, J. Zhu, L. Song, W. Zhang and Y. Xiong, *Adv. Mater.*, 2018, **30**, 1704624.
- 51 J. Di, C. Chen, S. Z. Yang, S. Chen, M. Duan, J. Xiong, C. Zhu, R. Long, W. Hao, Z. Chi, H. Chen, Y. X. Weng, J. Xia, L. Song, S. Li, H. Li and Z. Liu, *Nat. Commun.*, 2019, **10**, 2840.
- 52 C. Xia, Y. Qiu, Y. Xia, P. Zhu, G. King, X. Zhang, Z. Wu, J. Y. T. Kim, D. A. Cullen, D. Zheng, P. Li, M. Shakouri, E. Heredia, P. Cui, H. N. Alshareef, Y. Hu and H. Wang, *Nat. Chem.*, 2021, **13**, 887–894.
- 53 G. Bae, H. Kim, H. Choi, P. Jeong, D. H. Kim, H. C. Kwon, K. S. Lee, M. Choi, H. S. Oh, F. Jaouen and C. H. Choi, *JACS Au*, 2021, **1**, 586–597.
- 54 Y. Jin, F. Lu, D. Yi, J. Li, F. Zhang, T. Sheng, F. Zhan, Y. n. Duan, G. Huang, J. Dong, B. Zhou, X. Wang and J. Yao, *CCS Chem.*, 2021, **3**, 1453–1462.
- 55 Y. Kwon, T. Y. Kim, G. Kwon, J. Yi and H. Lee, *J. Am. Chem. Soc.*, 2017, **139**, 17694–17699.
- 56 P. Zhou, H. Chen, Y. Chao, Q. Zhang, W. Zhang, F. Lv, L. Gu, Q. Zhao, N. Wang, J. Wang and S. Guo, *Nat. Commun.*, 2021, **12**, 4412.
- 57 S. Yang, J. Kim, Y. J. Tak, A. Soon and H. Lee, *Angew. Chem., Int. Ed.*, 2016, **55**, 2058–2062.
- 58 Y. Wang, J. Liu, Y. Wang, A. M. Al-Enizi and G. Zheng, *Small*, 2017, **13**, 1701809.
- 59 D. Liu, J. C. Liu, W. Cai, J. Ma, H. B. Yang, H. Xiao, J. Li, Y. Xiong, Y. Huang and B. Liu, *Nat. Commun.*, 2019, **10**, 1779.
- 60 M. Xiao, J. Zhu, G. Li, N. Li, S. Li, Z. P. Cano, L. Ma, P. Cui, P. Xu, G. Jiang, H. Jin, S. Wang, T. Wu, J. Lu, A. Yu, D. Su and Z. Chen, *Angew. Chem., Int. Ed.*, 2019, **58**, 9640–9645.
- 61 L. Nie, D. Mei, H. Xiong, B. Peng, Z. Ren, X. I. P. Hernandez, A. DeLaRiva, M. Wang, M. H. Engelhard, L. Kovarik, A. K. Datye and Y. Wang, *Science*, 2017, **358**, 1419–1423.
- 62 S. Back, J. Lim, N. Y. Kim, Y. H. Kim and Y. Jung, *Chem. Sci.*, 2017, **8**, 1090–1096.
- 63 Y. Xu, M. Chu, F. Liu, X. Wang, Y. Liu, M. Cao, J. Gong, J. Luo, H. Lin, Y. Li and Q. Zhang, *Nano Lett.*, 2020, **20**, 6865–6872.
- 64 I. Roger, M. A. Shipman and M. D. Symes, *Nat. Rev. Chem.*, 2017, **1**, 0003.
- 65 J. L. White, M. F. Baruch, J. E. Pander III, Y. Hu, I. C. Fortmeyer, J. E. Park, T. Zhang, K. Liao, J. Gu, Y. Yan, T. W. Shaw, E. Abelev and A. B. Bocarsly, *Chem. Rev.*, 2015, **115**, 12888–12935.
- 66 B. Xia, Y. Zhang, J. Ran, M. Jaroniec and S. Z. Qiao, *ACS Cent. Sci.*, 2021, **7**, 39–54.
- 67 S. K. Kaiser, Z. Chen, D. Faust Akl, S. Mitchell and J. Perez-Ramirez, *Chem. Rev.*, 2020, **120**, 11703–11809.
- 68 C. Zhu, S. Fu, Q. Shi, D. Du and Y. Lin, *Angew. Chem., Int. Ed.*, 2017, **56**, 13944–13960.
- 69 G. Yang, Y. Li, H. Lin, X. Ren, D. Philo, Q. Wang, Y. He, F. Ichihara, S. Luo, S. Wang and J. Ye, *Small Methods*, 2020, **4**, 2000577.
- 70 Y. Qin, J. Wen, L. Zheng, H. Yan, L. Jiao, X. Wang, X. Cai, Y. Wu, G. Chen, L. Chen, L. Hu, W. Gu and C. Zhu, *Nano Lett.*, 2021, **21**, 1879–1887.
- 71 J. Zhang, G. Zhang, H. Lan, H. Liu and J. Qu, *Chem. Eng. J.*, 2022, **428**, 130373.
- 72 T. Wang, L. Guo, H. Pei, S. Chen, R. Li, J. Zhang and T. Peng, *Small*, 2021, 2102957.

- 73 W. Wang, S. Zhang, Y. Liu, L.-R. Zheng, G. Wang, Y. Zhang, H. Zhang and H. Zhao, *Chin. Chem. Lett.*, 2021, **32**, 805–810.
- 74 Y. C. Hao, L. W. Chen, J. Li, Y. Guo, X. Su, M. Shu, Q. Zhang, W. Y. Gao, S. Li, Z. L. Yu, L. Gu, X. Feng, A. X. Yin, R. Si, Y. W. Zhang, B. Wang and C. H. Yan, *Nat. Commun.*, 2021, **12**, 2682.
- 75 Y. Wang, X. Zhao, D. Cao, Y. Wang and Y. Zhu, *Appl. Catal., B*, 2017, **211**, 79–88.
- 76 F. Wang, Y. Wang, Y. Feng, Y. Zeng, Z. Xie, Q. Zhang, Y. Su, P. Chen, Y. Liu, K. Yao, W. Lv and G. Liu, *Appl. Catal., B*, 2018, **221**, 510–520.
- 77 L. Yi, F. Lan, J. Li and C. Zhao, *ACS Sustainable Chem. Eng.*, 2018, **6**, 12766–12775.
- 78 J. Li, H. Huang, P. Liu, X. Song, D. Mei, Y. Tang, X. Wang and C. Zhong, *J. Catal.*, 2019, **375**, 351–360.
- 79 X. H. Jiang, L. S. Zhang, H. Y. Liu, D. S. Wu, F. Y. Wu, L. Tian, L. L. Liu, J. P. Zou, S. L. Luo and B. B. Chen, *Angew. Chem., Int. Ed.*, 2020, **59**, 23112–23116.
- 80 Z. Zeng, Y. Su, X. Quan, W. Choi, G. Zhang, N. Liu, B. Kim, S. Chen, H. Yu and S. Zhang, *Nano Energy*, 2020, **69**, 104409.
- 81 M. Kou, W. Liu, Y. Wang, J. Huang, Y. Chen, Y. Zhou, Y. Chen, M. Ma, K. Lei, H. Xie, P. K. Wong and L. Ye, *Appl. Catal., B*, 2021, **291**, 120146.
- 82 J.-H. Zhang, W. Yang, M. Zhang, H.-J. Wang, R. Si, D.-C. Zhong and T.-B. Lu, *Nano Energy*, 2021, **80**, 105542.
- 83 Z. Han, Y. Zhao, G. Gao, W. Zhang, Y. Qu, H. Zhu, P. Zhu and G. Wang, *Small*, 2021, **17**, 2102089.
- 84 J. Deng, Y. Su, D. Liu, P. Yang, B. Liu and C. Liu, *Chem. Rev.*, 2019, **119**, 9221–9259.
- 85 H. V. Thang, G. Pacchioni, L. DeRita and P. Christopher, *J. Catal.*, 2018, **367**, 104–114.
- 86 B. Han, R. Lang, H. Tang, J. Xu, X.-K. Gu, B. Qiao and J. Liu, *Chin. J. Catal.*, 2019, **40**, 1847–1853.
- 87 R. Gao, J. Wang, Z.-F. Huang, R. Zhang, W. Wang, L. Pan, J. Zhang, W. Zhu, X. Zhang, C. Shi, J. Lim and J.-J. Zou, *Nat. Energy*, 2021, **6**, 614–623.
- 88 J. Park, S. Lee, H. E. Kim, A. Cho, S. Kim, Y. Ye, J. W. Han, H. Lee, J. H. Jang and J. Lee, *Angew. Chem., Int. Ed.*, 2019, **58**, 16038–16042.
- 89 G. Cha, I. Hwang, S. Hejazi, A. S. Dobrota, I. A. Pasti, B. Osuagwu, H. Kim, J. Will, T. Yokosawa, Z. Badura, S. Kment, S. Mohajernia, A. Mazare, N. V. Skorodumova, E. Spiecker and P. Schmuki, *iScience*, 2021, **24**, 102938.
- 90 D. Lebedev, R. Ezhov, J. Heras-Domingo, A. Comas-Vives, N. Kaeffer, M. Willinger, X. Solans-Monfort, X. Huang, Y. Pushkar and C. Copéret, *ACS Cent. Sci.*, 2020, **6**, 1189–1198.
- 91 C. Cheng, W. H. Fang, R. Long and O. V. Prezhdo, *JACS Au*, 2021, **1**, 550–559.
- 92 L. Zeng, C. Dai, B. Liu and C. Xue, *J. Mater. Chem. A*, 2019, **7**, 24217–24221.
- 93 J. N. Tiwari, A. N. Singh, S. Sultan and K. S. Kim, *Adv. Energy Mater.*, 2020, **10**, 2000280.
- 94 M. B. Gawande, P. Fornasiero and R. Zbořil, *ACS Catal.*, 2020, **10**, 2231–2259.
- 95 T. Sun, L. Xu, D. Wang and Y. Li, *Nano Res.*, 2019, **12**, 2067–2080.
- 96 S. Verma, S. Lu and P. J. A. Kenis, *Nat. Energy*, 2019, **4**, 466–474.
- 97 Y. Shi, C. Zhao, H. Wei, J. Guo, S. Liang, A. Wang, T. Zhang, J. Liu and T. Ma, *Adv. Mater.*, 2014, **26**, 8147–8153.
- 98 N. Li, C. Zhu, J. Zhang, H. Jing, J. Hu, C. Hao and Y. Shi, *Chem. Commun.*, 2021, **57**, 5302–5305.
- 99 H. T. Lien, S. T. Chang, P. T. Chen, D. P. Wong, Y. C. Chang, Y. R. Lu, C. L. Dong, C. H. Wang, K. H. Chen and L. C. Chen, *Nat. Commun.*, 2020, **11**, 4233.
- 100 J. Jones, H. Xiong, A. T. DeLaRiva, E. J. Peterson, H. Pham, S. R. Challa, G. Qi, S. Oh, M. H. Wiebenga, X. I. Pereira Hernandez, Y. Wang and A. K. Datye, *Science*, 2016, **353**, 150–154.